# Evidence for Heavy Hyperhydrogen $^6_\Lambda$H

M. Agnello,[1,2] L. Benussi,[3] M. Bertani,[3] H. C. Bhang,[4] G. Bonomi,[5,6] E. Botta,[7,2,*] M. Bregant,[8] T. Bressani,[7,2]
S. Bufalino,[2] L. Busso,[9,2] D. Calvo,[2] P. Camerini,[10,11] B. Dalena,[12] F. De Mori,[7,2] G. D'Erasmo,[13,14] F. L. Fabbri,[3]
A. Feliciello,[2] A. Filippi,[2] E. M. Fiore,[13,14] A. Fontana,[6] H. Fujioka,[15] P. Genova,[6] P. Gianotti,[3] N. Grion,[10] V. Lucherini,[3]
S. Marcello,[7,2] N. Mirfakhrai,[16] F. Moia,[5,6] O. Morra,[17,2] T. Nagae,[15] H. Outa,[18] A. Pantaleo,[14,†] V. Paticchio,[14] S. Piano,[10]
R. Rui,[10,11] G. Simonetti,[13,14] R. Wheadon,[2] and A. Zenoni[5,6]

(FINUDA Collaboration)

[1]*Dipartimento di Fisica, Politecnico di Torino, Corso Duca degli Abruzzi 24, Torino, Italy*
[2]*INFN Sezione di Torino, via P. Giuria 1, Torino, Italy*
[3]*Laboratori Nazionali di Frascati dell'INFN, via E. Fermi 40, Frascati, Italy*
[4]*Department of Physics, Seoul National University, 151-742 Seoul, South Korea*
[5]*Dipartimento di Ingegneria Meccanica e Industriale, Università di Brescia, via Valotti 9, Brescia, Italy*
[6]*INFN Sezione di Pavia, via Bassi 6, Pavia, Italy*
[7]*Dipartimento di Fisica Sperimentale, Università di Torino, Via P. Giuria 1, Torino, Italy*
[8]*SUBATECH, École des Mines de Nantes, Université de Nantes, CNRS-IN2P3, Nantes, France*
[9]*Dipartimento di Fisica Generale, Università di Torino, Via P. Giuria 1, Torino, Italy*
[10]*INFN Sezione di Trieste, via Valerio 2, Trieste, Italy*
[11]*Dipartimento di Fisica, Università di Trieste, via Valerio 2, Trieste, Italy*
[12]*CEA, Irfu/SACM, Gif-sur-Yvette, France*
[13]*Dipartimento di Fisica Università di Bari, via Amendola 173, Bari, Italy*
[14]*INFN Sezione di Bari, via Amendola 173, Bari, Italy*
[15]*Department of Physics, Kyoto University, Sakyo-ku, Kyoto, Japan*
[16]*Department of Physics, Shahid Behesty University, 19834 Teheran, Iran*
[17]*INAF-IFSI, Sezione di Torino, Corso Fiume 4, Torino, Italy*
[18]*RIKEN, Wako, Saitama 351-0198, Japan*

A. Gal

*Racah Institute of Physics, The Hebrew University, Jerusalem 91904, Israel*
(Received 2 November 2011; published 24 January 2012)

Evidence for the neutron-rich hypernucleus $^6_\Lambda$H is presented from the FINUDA experiment at DAΦNE, Frascati, studying $(\pi^+, \pi^-)$ pairs in coincidence from the $K^-_{stop} + {}^6\text{Li} \rightarrow {}^6_\Lambda\text{H} + \pi^+$ production reaction followed by $^6_\Lambda\text{H} \rightarrow {}^6\text{He} + \pi^-$ weak decay. The production rate of $^6_\Lambda$H undergoing this two-body $\pi^-$ decay is determined to be $(2.9 \pm 2.0) \times 10^{-6}/K^-_{stop}$. Its binding energy, evaluated jointly from production and decay, is $B_\Lambda(^6_\Lambda\text{H}) = (4.0 \pm 1.1)$ MeV with respect to $^5\text{H} + \Lambda$. A systematic difference of $(0.98 \pm 0.74)$ MeV between $B_\Lambda$ values derived separately from decay and from production is tentatively assigned to the $^6_\Lambda\text{H}\ 0^+_{\text{g.s.}} \rightarrow 1^+$ excitation.

*Introduction.*—The existence and observability of neutron-rich $\Lambda$ hypernuclei was discussed back in 1963 by Dalitz and Levi-Setti [1], who predicted the stability of $^6_\Lambda$H consisting of four neutrons, one proton, and one $\Lambda$ hyperon. Accordingly, the $\Lambda$ hyperon stabilizes the core nucleus $^5$H, which is a broad resonance 1.7 MeV above $^3\text{H} + 2n$ [2]. To be stable, $^6_\Lambda$H must lie also below $^4_\Lambda\text{H} + 2n$, which provides the lowest particle stability threshold. This motivates a $^4_\Lambda\text{H} + 2n$ two-neutron halo cluster structure for $^6_\Lambda$H, with a binding energy and excitation spectrum that might deviate substantially from the extrapolation practiced in Ref. [1]. Specifically, the study of $^6_\Lambda$H and of heavier neutron-rich hypernuclei that go appreciably be-

yond the neutron stability drip line in nuclear systems could place valuable constraints on the size of coherent $\Lambda N - \Sigma N$ mixing in dense strange neutron-rich matter [3]. This mixing provides a robust mechanism for generating three-body $\Lambda NN$ interactions, with an immediate impact on the stiffness or softness of the equation of state for hyperons in neutron-star matter, as reviewed recently in Ref. [4].

In this Letter, we report on a study of $^6_\Lambda$H in the double charge exchange reaction at rest

$$K^-_{stop} + {}^6\text{Li} \rightarrow {}^6_\Lambda\text{H} + \pi^+ (p_{\pi^+} \sim 252 \text{ MeV}/c) \quad (1)$$

based on analyzing the total data sample of the FINUDA experiment during 2003–2007 and corresponding to a total integrated luminosity of 1156 pb$^{-1}$. A first analysis of the partial data, corresponding to an integrated luminosity 190 pb$^{-1}$, gave only an upper limit for (1): $(2.5 \pm 0.4_{\mathrm{stat}-0.1\mathrm{syst}}^{+0.4}) \times 10^{-5}/K_{\mathrm{stop}}^{-}$ [5]. Although the statistics collected on $^6$Li targets is improved by a factor of 5 with respect to the run of the earlier search, the inclusive $\pi^+$ spectra do not show any clear peak attributable to $^6_\Lambda$H near $p_{\pi^+} \sim 252$ MeV/$c$. Exploiting the increased statistics, the essential idea of the present analysis was to reduce the overwhelming background events in reaction (1) by requiring a coincidence with $\pi^-$ mesons from the two-body weak decay

$$^6_\Lambda\mathrm{H} \rightarrow {}^6\mathrm{He} + \pi^- (p_{\pi^-} \sim 134 \text{ MeV}/c), \quad (2)$$

with a branching ratio of about 50% considering the value measured for $^4_\Lambda\mathrm{H} \rightarrow {}^4\mathrm{He} + \pi^-$ [6]. The analysis described below yielded three distinct $^6_\Lambda$H candidate events which give evidence for a particle-stable $^6_\Lambda$H with some indication of its excitation spectrum. The deduced $^6_\Lambda$H binding energy does not confirm the large effects conjectured in Ref. [3].

*Data analysis.*—We first recall the experimental features relevant to the present analysis. For $\pi^+$ with momentum $\sim 250$ MeV/$c$, the resolution of the tracker was determined by means of the peak due to monochromatic (236.5 MeV/$c$) $\mu^+$ from $K_{\mu 2}$ decay and is $\sigma_p = (1.1 \pm 0.1)$ MeV/$c$ [7]; the precision on the absolute momentum calibration is better than 0.12 MeV/$c$ for the $^6$Li targets, which corresponds to a systematic deviation on the kinetic energy $\sigma_{T\mathrm{syst}}(\pi^+) = 0.1$ MeV. For $\pi^-$ with momentum $\sim 130$ MeV/$c$, the resolution and absolute calibration were evaluated from the peak due to monochromatic (132.8 MeV/$c$) $\pi^-$ coming from the two-body weak decay of $^4_\Lambda$H, produced as a hyperfragment with a formation probability of about $10^{-3}$–$10^{-2}$ per stopped $K^-$ [6]. A resolution $\sigma_p = (1.2 \pm 0.1)$ MeV/$c$ and a precision of 0.2 MeV/$c$ were found, corresponding to a systematic deviation of the kinetic energy $\sigma_{T\mathrm{syst}}(\pi^-) = 0.14$ MeV.

Since the stopping time of $^6_\Lambda$H in metallic Li is shorter than its lifetime, both production (1) and decay (2) occur at rest, and a straightforward algebra leads to the following expression for $T_{\mathrm{sum}} \equiv T(\pi^+) + T(\pi^-)$:

$$T_{\mathrm{sum}} = M(K^-) + M(p) - M(n) - 2M(\pi) - B(^6\mathrm{Li})$$
$$+ B(^6\mathrm{He}) - T(^6\mathrm{He}) - T(^6_\Lambda\mathrm{H}), \quad (3)$$

in which $M$ stands for known masses, $B$ for known nuclear binding energies, and $T$ for kinetic energies. The evaluation of $T(^6_\Lambda\mathrm{H})$ using momentum and energy conservation depends explicitly on the knowledge of $B_\Lambda(^6_\Lambda\mathrm{H})$, whereas $T(^6\mathrm{He})$ depends only implicitly on $B_\Lambda(^6_\Lambda\mathrm{H})$ through the momentum $p_{\pi^-}$.

We assume $B_\Lambda(^6_\Lambda\mathrm{H}) = 5$ MeV, the average of 4.2 and 5.8 MeV predicted in Refs. [1,3], respectively, with respect to $^5\mathrm{H} + \Lambda$. This choice is not critical, since $T_{\mathrm{sum}}$ varies merely by 50 keV upon varying $B_\Lambda(^6_\Lambda\mathrm{H})$ by 1 MeV, negligibly low with respect to the experimental energy resolutions $\sigma_T(\pi^+) = 0.96$ MeV and $\sigma_T(\pi^-) = 0.84$ MeV for $p_{\pi^+} \approx 250$ MeV/$c$ and $p_{\pi^-} \approx 130$ MeV/$c$. Therefore, the FINUDA energy resolution for a $\pi^\pm$ pair in coincidence is $\sigma_T = 1.28$ MeV. Evaluating the right-hand side (RHS) of Eq. (3), one obtains $T_{\mathrm{sum}} = 203 \pm 1.3$ MeV for $^6_\Lambda$H candidate events. In practice, we have focused on events in the interval $T_{\mathrm{sum}} = 203 \pm 1$ MeV, corresponding to only $\sim 77\%$ of the FINUDA total energy resolution; this value was chosen as a compromise between seeking to reduce contamination from background reactions, discussed in more detail below, and maintaining reasonable statistics, which resulted in a somewhat narrower interval than the experimental resolution. The raw spectrum of $T_{\mathrm{sum}}$ for $\pi^\pm$ pair coincidence events is shown in Fig. 1, where events satisfying $T_{\mathrm{sum}} = 203 \pm 1$ MeV are indicated by a vertical (red) bar.

Figure 2 (left) shows a 2D plot in the $p_{\pi^\pm}$ plane of coincidence events selected in the band $T_{\mathrm{sum}} = 202$–$204$ MeV. The distribution falls to zero at $p_{\pi^+} \simeq 245$ MeV/$c$ and higher and at $p_{\pi^-} \simeq 145$ MeV/$c$ and lower. This is close to where $^6_\Lambda$H events are expected. Thus, to search for particle-stable $^6_\Lambda$H events below its $(^4_\Lambda\mathrm{H} + 2n)$ lowest threshold, by using the two-body kinematics of Eqs. (1) and (2), a further requirement of $p_{\pi^+} > 251.9$ MeV/$c$ and $p_{\pi^-} < 135.6$ MeV/$c$ is necessary. In the final analysis we selected $p_{\pi^+} = (250$–$255)$ MeV/$c$
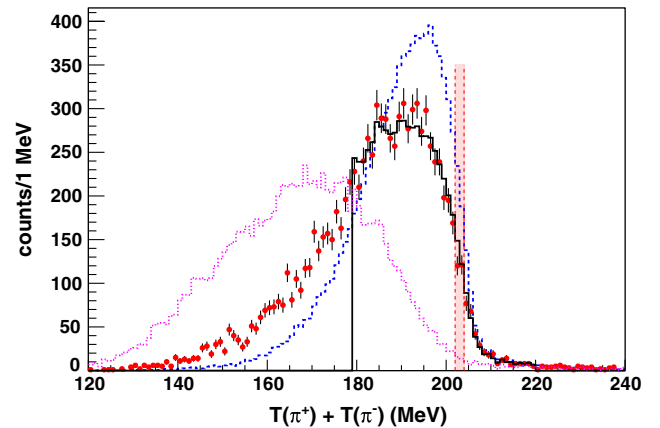


FIG. 1 (color online). Distribution of raw total kinetic energy $T_{\mathrm{sum}} \equiv T(\pi^+) + T(\pi^-)$ for $\pi^\pm$ pair coincidence events from $^6$Li targets. The vertical (red) bar represents the cut $T_{\mathrm{sum}} = 202$–$204$ MeV. The dashed (blue) histogram is a quasifree simulation of $K_{\mathrm{stop}}^- + {}^6\mathrm{Li} \rightarrow \Sigma^+ + {}^4\mathrm{He} + n + \pi^-$; $\Sigma^+ \rightarrow n + \pi^+$ background, and the dotted (violet) histogram is a four-body phase space simulation of the same background. Their best fit to the data is shown by the solid (black) histogram; see the text.
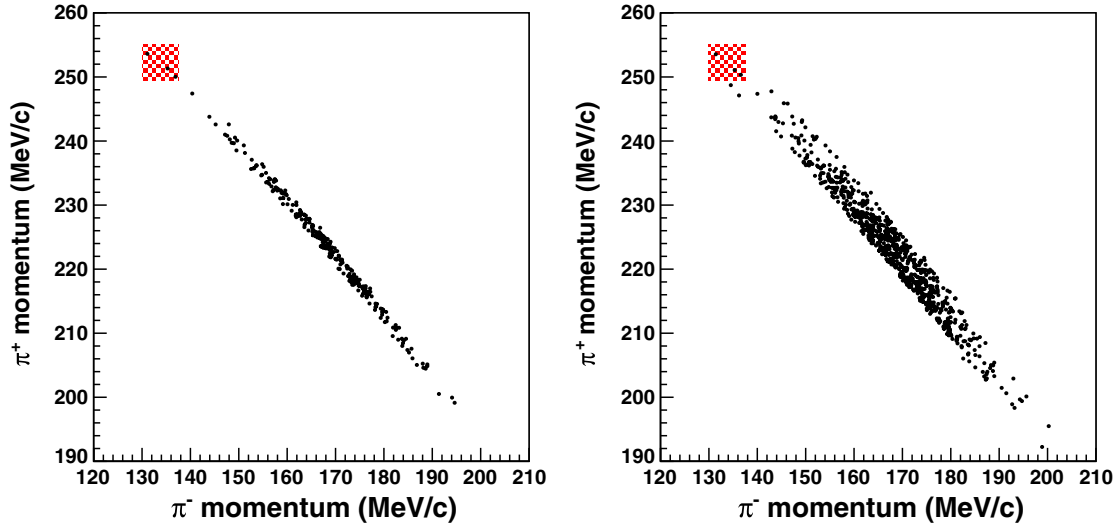
FIG. 2 (color online). $\pi^+$ momentum vs $\pi^-$ momentum for $^6$Li target events with $T_{\rm sum} = 202$–204 MeV (LHS) and with $T_{\rm sum} = 200$–206 MeV (RHS). The shaded (red) rectangle on each side consists of a subset of events with $p_{\pi^+} = 250$–255 MeV$/c$ and $p_{\pi^-} = 130$–137 MeV$/c$.

and $p_{\pi^-} = (130$–137$)$ MeV$/c$, thus covering a $^6_\Lambda$H mass range from the $(\Lambda + {}^3{\rm H} + 2n)$ threshold, about 2 MeV in the $^6_\Lambda$H continuum, down to a $^6_\Lambda$H bound somewhat stronger than predicted by Akaishi *et al.* [3]. This does not completely exclude eventual contributions from the production and decay of $(^4_\Lambda{\rm H} + 2n)$ as discussed below.

*Results.*—Out of a total number of $\sim 2.7 \times 10^7$ $K^-$ detected at stop in the $^6$Li targets, we found three events that satisfy the final requirements: $T_{\rm sum} = 202$–204 MeV, $p_{\pi^+} = 250$–255 MeV$/c$, and $p_{\pi^-} = 130$–137 MeV$/c$, as shown within the shaded (red) rectangle in Fig. 2 (left). Different choices of $T_{\rm sum}$ interval widths (2–6 MeV) and position (center in 202–204 MeV) and of $p_{\pi^\pm}$ interval widths (5–10 and 8–15 MeV$/c$, respectively) with fixed limits at 250 and 137 MeV$/c$, respectively, to exclude the unbound region do not affect the population of this selected rectangle. For example, no new candidate events appear in the shaded rectangle upon extending the cut $T_{\rm sum} = 202$–204 MeV in the left-hand side (LHS) of Fig. 2 to $T_{\rm sum} = 200$–206 MeV in the RHS of the figure. A similar stability is not observed in the opposite corner of Fig. 2, where, on top of the events already there on the LHS, six additional events appear on the RHS upon extending the $T_{\rm sum}$ cut of the LHS. Quantitatively, by fitting the projected $\pi^\pm$ distributions of Fig. 2 left by Gaussians, an excess of three events in both $p_{\pi^\pm}$ distributions is invariably found,

corresponding to the shaded (red) rectangle. The probability for the three events to belong to the fitted Gaussian distribution is less than 0.5% in both cases. This rules out systematic errors associated with the present analysis selection.

The three $^6_\Lambda$H candidate events are listed in Table I together with nuclear mass values derived separately from production (1) and from decay (2). These mass values yield a mean value $M(^6_\Lambda{\rm H}) = 5801.4 \pm 1.1$ MeV, jointly from production and decay, where the error reflects the spread of the average mass values for the three events and is larger than the 0.96 and 0.84 MeV measurement uncertainties in production and decay, respectively, for each of the three events. We note that the mass value inferred from the third event by averaging on production and decay is about $2\sigma$ from the mean mass value, an observation that could indicate some irregularity in the reconstruction of the third event. To regain confidence, each one of the three events was checked visually for irregularities, but none was found.

Furthermore, we note from Table I that the mass values associated with production are systematically higher than those associated with decay, by $0.98 \pm 0.74$ MeV recalling the 1.28 MeV uncertainty for $T_{\rm sum}$ from which each of these mass differences is directly determined. Unlike the mean $^6_\Lambda$H mass value, the spread of the production vs decay mass differences is well within $1\sigma$. These mass differences

TABLE I. Summed kinetic energy $T_{\rm sum} = T(\pi^+) + T(\pi^-)$, pion momenta $p_{\pi^\pm}$, and mass values inferred for the three $^6_\Lambda$H candidate events from production (1) and decay (2). The mean mass value is $M(^6_\Lambda{\rm H}) = 5801.4 \pm 1.1$ MeV; see the text.

| $T_{\rm sum}$ (MeV) | $p_{\pi^+}$ (MeV$/c$) | $p_{\pi^-}$ (MeV$/c$) | $M(^6_\Lambda{\rm H})_{\rm prod.}$ (MeV) | $M(^6_\Lambda{\rm H})_{\rm decay}$ (MeV) |
|---|---|---|---|---|
| $202.6 \pm 1.3$ | $251.3 \pm 1.1$ | $135.1 \pm 1.2$ | $5802.33 \pm 0.96$ | $5801.41 \pm 0.84$ |
| $202.7 \pm 1.3$ | $250.1 \pm 1.1$ | $136.9 \pm 1.2$ | $5803.45 \pm 0.96$ | $5802.73 \pm 0.84$ |
| $202.1 \pm 1.3$ | $253.8 \pm 1.1$ | $131.2 \pm 1.2$ | $5799.97 \pm 0.96$ | $5798.66 \pm 0.84$ |

are likely to be connected to the excitation spectrum of $^6_\Lambda$H as discussed below.

*Background estimate and production rate.*—A complete simulation was performed of $K^-_{stop}$ absorption reactions on single nucleons, as well as on correlated few-nucleon clusters, that lead to the formation and decay of $\Lambda$ and $\Sigma$ hyperons. Full details will be given elsewhere; here, it is sufficient to focus on two chains of reactions likely to produce $\pi^\pm$ coincidences overlapping with those selected to satisfy $^6_\Lambda$H production (1) and decay (2).

(i) $\Sigma^+$ production:

$$K^-_{stop} + {}^6\text{Li} \rightarrow \Sigma^+ + {}^4\text{He} + n + \pi^-, \qquad (4)$$

where $p_{\pi^-} \leq 190$ MeV/$c$, followed by $\Sigma^+$ decay in flight:

$$\Sigma^+ \rightarrow n + \pi^+ [p_{\pi^+} \leq 282 \text{ MeV}/c]. \qquad (5)$$
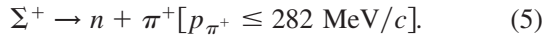
The $\Sigma^+$ production was treated in the quasifree approach, following the analysis of the FINUDA experiment observing $\Sigma^\pm \pi^\mp$ pairs [8]. This simulation is shown in Fig. 1, normalized to the experimental distribution area. It provides too sharp a decrease in the 200–210 MeV region. To have a satisfactory description, a contribution ($\sim 25\%$) from a pure four-body phase space mechanism was added and a fair agreement was obtained ($\chi^2 = 40/39$) in the 180–220 MeV range. The simulated background spectra reproduce reasonably the projected distributions of $\pi^\pm$ momentum too, showing, in particular, only a small contribution to the signal region, evaluated to be $0.16 \pm 0.07$ expected events (BGD1).

(ii) $^4_\Lambda$H production:

$$K^-_{stop} + {}^6\text{Li} \rightarrow {}^4_\Lambda\text{H} + 2n + \pi^+, \qquad (6)$$
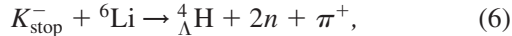
where $p_{\pi^+} \leq 252$ MeV/$c$, with $^4_\Lambda$H decay at rest:

$$^4_\Lambda\text{H} \rightarrow {}^4\text{He} + \pi^- [p_{\pi^-} \sim 132.8 \text{ MeV}/c]. \qquad (7)$$

The $\pi^-$ momentum in this $^4_\Lambda$H decay is close to $p_{\pi^-} \sim 134$ MeV/$c$ from the two-body decay of $^6_\Lambda$H, evaluated by assuming $B_\Lambda(^6_\Lambda\text{H}) = 5$ MeV as discussed above. A value of $0.04 \pm 0.01$ expected events for the (6) and (7) reaction chain, negligible when compared to BGD1, was obtained under most pessimistic assumptions for the various terms of the calculation.

All other reaction chains that could produce $\pi^\pm$ coincidences within the described selection ranges were ruled out by the selections applied. Turning to potential instrumental backgrounds, we note that these could result from fake tracks, misidentified as true events by the track reconstruction algorithms. To this end, we considered, with the same cuts, events coming from different nuclear targets used in the same runs ($^7$Li, $^9$Be, $^{13}$C, and $^{16}$O). We found one event coming from $^9$Be. Furthermore, we considered events relative to the $^6$Li targets, selected with a value of $T_{sum} = 193$–199 MeV, so as to search for neutron-rich hypernuclei

produced on the other targets. No event was found. We evaluate $0.27 \pm 0.27$ expected fake events from $^6$Li, due to instrumental background (BGD2).

To recap, the estimated number of events due to physical and instrumental backgrounds feeding through the selection criteria are $0.16 \pm 0.07$ (BGD1) and $0.27 \pm 0.27$ (BGD2), giving a total background of $0.43 \pm 0.28$ expected events. Thus, by using Poisson distribution, the three $^6_\Lambda$H-assigned events do not arise from the background to a confidence level of 99%. The statistical significance of the result is $S = 7.1$ considering only the physical background and $S = 3.9$ considering both physical and instrumental backgrounds.

Given the above background estimates, plus efficiency, target purity, and cut estimates, it is possible to evaluate the product $R(\pi^+)\text{BR}(\pi^-)$, where $R(\pi^+)$ is the $^6_\Lambda$H production rate per $K^-_{stop}$ in reaction (1) and $\text{BR}(\pi^-)$ the branching ratio for the two-body $\pi^-$ decay (2):

$$R(\pi^+)\text{BR}(\pi^-) = (2.9 \pm 2.0) \times 10^{-6}/K^-_{stop}. \qquad (8)$$

Details will be given in a separate report. Assuming $\text{BR}(\pi^-) = 49\%$, as for the analogous $^4_\Lambda\text{H} \rightarrow {}^4\text{He} + \pi^-$ decay [6], we find $R(\pi^+) = (5.9 \pm 4.0) \times 10^{-6}/K^-_{stop}$, fully consistent with the previous FINUDA upper limit [5].

*Discussion and conclusion.*—Table I yields a mean value $B_\Lambda(^6_\Lambda\text{H}) = 4.0 \pm 1.1$ MeV with respect to $^5\text{H} + \Lambda$, as shown in Fig. 3, in good agreement with the estimate 4.2 MeV [1] and close to $B_\Lambda(^6_\Lambda\text{He}) = 4.18 \pm 0.10$ MeV (with respect to $^5\text{He} + \Lambda$) for the other known $A = 6$ hypernucleus [9] but considerably short of Akaishi's prediction $B^{th}_\Lambda(^6_\Lambda\text{H}) = 5.8$ MeV [3]. This indicates that coherent $\Lambda N - \Sigma N$ mixing in the $s$-shell hypernucleus $^4_\Lambda$H [10] becomes rather ineffective for the excess $p$-shell neutrons in $^6_\Lambda$H. Indeed, recent shell-model calculations by Millener indicate that $\Lambda N - \Sigma N$ mixing contributions to $B_\Lambda$ and to doublet spin splittings in the $p$ shell are rather small, about $(10 \pm 5)\%$ of their contribution in $^4_\Lambda$H [11].

Next, we ask whether the three events that give evidence for a particle-stable $^6_\Lambda$H provide additional information on
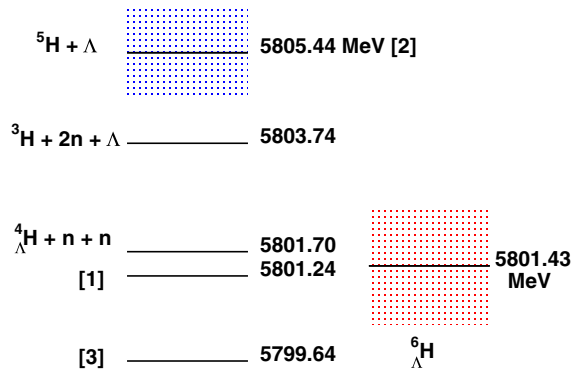


FIG. 3 (color online). $^6_\Lambda$H mass (RHS) from three $^6_\Lambda$H candidate events, as related to several particle stability thresholds and theoretical predictions (LHS).

its excitation spectrum which is expected to consist of a $0^+$ ground state (g.s.) and $1^+$ excited state as in $^4_\Lambda$H (1.04 MeV) and a $2^+$ excited state as for the $p$-shell dineutron system in $^6$He (1.80 MeV). In fact, it is $^6_\Lambda$H($1^+$) that is likely to be produced in reaction (1) simply because Pauli spin is conserved in production at rest, and the Pauli spin of $^6$Li is $S = 1$ to better than 98% [11]. The weak decay (2), however, occurs from the $^6_\Lambda$H($0^+$) g.s. since the (unseen) $\gamma$ transition $1^+ \rightarrow 0^+$ is about 3 orders of magnitude faster than weak decay. Indeed, the production vs decay mass difference $0.98 \pm 0.74$ MeV extracted from the three $^6_\Lambda$H events listed in Table I is comparable to the underlying 1.04 MeV $1^+$ excitation in $^4_\Lambda$H but, again, smaller than the 2.4 MeV predicted by Akaishi *et al.* [3]. If this is the case, then the $B_\Lambda$ value for the g.s. would be larger by 0.5 MeV than that determined above, amounting to $B_\Lambda(^6_\Lambda H_{\mathrm{g.s.}}) = 4.5 \pm 1.2$ MeV. This scenario requires further exploration, experimental as well as theoretical.

In conclusion, we have presented the first evidence for heavy hyperhydrogen $^6_\Lambda$H, based on detecting three events shown to be clear of instrumental and/or physical backgrounds. The derived binding energy of $^6_\Lambda$H limits the strength of the coherent $\Lambda N - \Sigma N$ mixing effect predicted in neutron-rich strange matter [3], and together with the conjectured $0^+ - 1^+$ doublet splitting it places a limit on this mixing that could orient further explorations of other neutron-rich hypernuclei. A search of $^6_\Lambda$H and $^{10}_\Lambda$Li in the $(\pi^-, K^+)$ reaction at 1.2 GeV/$c$ on $^6$Li and $^{10}$B, respectively, is scheduled in the near future at Japan Proton Accelerator Research Complex.

*Corresponding author.
botta@to.infn.it
†Deceased.

[1] R. H. Dalitz and R. Levi-Setti, Nuovo Cimento **30**, 489 (1963); L. Majling, Nucl. Phys. **A585**, 211c (1995).
[2] A. A. Korsheninnikov *et al.*, Phys. Rev. Lett. **87**, 092501 (2001).
[3] Y. Akaishi and T. Yamazaki, in *Physics and Detectors for DAΦNE*, Frascati Physics Series Vol. 16 (SIS INFN-LNF, Rome, 1999), p. 59; S. Shinmura, K. S. Myint, T. Harada, and Y. Akaishi, J. Phys. G **28**, L1 (2002); for a recent review, see Y. Akaishi and K. S. Myint, AIP Conf. Proc. **1011**, 277 (2008); Y. Akaishi, Prog. Theor. Phys. Suppl. **186**, 378 (2010), and references therein.
[4] J. Schaffner-Bielich, Nucl. Phys. **A804**, 309 (2008); **A835**, 279 (2010).
[5] M. Agnello *et al.*, Phys. Lett. B **640**, 145 (2006), including a detailed description of the FINUDA experiment, in particular, for the $(K^-_{\mathrm{stop}}, \pi^+)$ production reaction.
[6] H. Tamura *et al.*, Phys. Rev. C **40**, R479 (1989).
[7] M. Agnello *et al.*, Phys. Lett. B **698**, 219 (2011).
[8] M. Agnello *et al.*, Phys. Lett. B **704**, 474 (2011).
[9] D. H. Davis, Nucl. Phys. **A754**, 3 (2005).
[10] Y. Akaishi, T. Harada, S. Shinmura, and K. S. Myint, Phys. Rev. Lett. **84**, 3539 (2000).
[11] D. J. Millener, Lect. Notes Phys. **724**, 31 (2007), and references therein.